The Journal of Chemical Physics

Semiclassical description of nuclear dynamics moving through complex-valued single avoided crossings of two electronic states

Cite as: J. Chem. Phys. **154**, 234101 (2021); https://doi.org/10.1063/5.0054014
Submitted: 13 April 2021 . Accepted: 25 May 2021 . Published Online: 16 June 2021

Yanze Wu and Joseph E. Subotnik

The Journal of Chemical Physics ARTICLE scitation.org/journal/jcp

Semiclassical description of nuclear dynamics moving through complex-valued single avoided crossings of two electronic states

Cite as: J. Chem. Phys. 154, 234101 (2021); doi: 10.1063/5.0054014
Submitted: 13 April 2021 • Accepted: 25 May 2021 •
Published Online: 16 June 2021

Yanze Wu[a] and Joseph E. Subotnik[b]

AFFILIATIONS

Department of Chemistry, University of Pennsylvania, Philadelphia, Pennsylvania 19104, USA

[a]wuyanze@sas.upenn.edu
[b]Author to whom correspondence should be addressed: subotnik@sas.upenn.edu

ABSTRACT

The standard fewest-switches surface hopping (FSSH) approach fails to model nonadiabatic dynamics when the electronic Hamiltonian is complex-valued and there are multiple nuclear dimensions; FSSH does not include geometric magnetic effects and does not have access to a gauge independent direction for momentum rescaling. In this paper, for the case of a Hamiltonian with two electronic states, we propose an extension of Tully's FSSH algorithm, which includes geometric magnetic forces and, through diabatization, establishes a well-defined rescaling direction. When combined with a decoherence correction, our new algorithm shows satisfying results for a model set of two-dimensional single avoided crossings.

I. INTRODUCTION

Nonadiabatic dynamics are one of the most important phenomena in chemical dynamics, playing a crucial role in many chemical reactions, especially those involving photo-excitation.[1–4] During nonadiabatic transitions, the electronic wavefunction changes rapidly, accompanied by a conversion of electronic energy into nuclear kinetic energy. Because of the importance of the problem, physical chemists are always seeking new and intuitive theories of nonadiabatic transitions. In particular, for several decades, theorists have searched (and continue to search) for the optimal semiclassical approach to describe nonadiabatic transitions, with nuclei treated classically and electrons treated quantum-mechanically. Whenever quantum phenomena arise with respect to the electronic motion, some feedback mechanism will necessarily arise as far as the nuclear motion is concerned and there is no unique means of determining that feedback classically.[5,6]

One quantum phenomenon that can arise within the scope of nonadiabatic dynamics is the presence of spin–orbit coupling, which causes the electronic Hamiltonian to be complex-valued. In such a case, as shown by Berry and Robbins,[7] nuclei no longer follow Newtonian trajectories but rather experience an extra "geometric magnetic force" (or Berry force), which arises from the curvature of the geometric phase.[8,9] In the adiabatic limit, the analytical expression for Berry force is[7]

$$\mathbf{F}_j^B = \frac{2\hbar}{M}\sum_k \mathrm{Im}\{(\mathbf{P}\cdot\mathbf{d}_{kj})\mathbf{d}_{jk}\}, \tag{1}$$

where j is the active adiabat, $\mathbf{P}$ is the nuclear momentum, and $\mathbf{d}_{kj}$ is the derivative coupling between adiabat k and j. Recent studies have shown that such geometric magnetism can cause spin polarization[10,11] and may underlie a wide variety of spin related phenomena, such as chirality induced spin selectivity (CISS).[12,13]

To date, there are a very limited number of literature studies merging semiclassical methods with complex-valued Hamiltonians (with Berry force). The usual candidates for semiclassical methods [Ehrenfest dynamics,[14] fewest-switches surface hopping (FSSH),[15] and *ab initio* multiple spawning (AIMS)[16,17]] have heretofore been applied almost entirely to problems where the Hamiltonians are real-valued (i.e., problems without spin–orbit coupling). In addition, in cases where FSSH has been applied to intersystem crossings, Berry

force has been neglected.[2–4,18] In practice, we have found (and as will be clear below) that generalizing the standard methods above to accurately account for complex-valued Hamiltonians and geometric magnetism turns out to be a non-trivial task. On the one hand, as far as mean-field approaches are concerned, while Ehrenfest dynamics does include (by default) geometric magnetism in its equations of motion,[9] the method suffers from a lack of path branching, decoherence,[19–21] and detailed balance.[22,23] As a result, we have found that standard Ehrenfest dynamics cannot describe many of the most interesting features of nonadiabatic theory in the presence of strong Berry force effects (e.g., strong non-Condon spin–orbit coupling effects[24]). While we have empirically found some encouraging results with quasiclassical trajectories (that included electronic zero point energy), we have not yet been able to fashion a stable algorithm [e.g., in the spirit of Cotton and Miller's symmetric quasiclassical (SQC) approach[25]] to accurately treat nonadiabatic dynamics with complex-valued Hamiltonians. We have not yet tested other mean-field inspired algorithms [e.g., forward–backward trajectories[26] and partial linearized density matrix (PLDM)[27,28]] to ascertain how these methods perform with complex-valued Hamiltonians.

On the other hand, as far as stochastic algorithms are concerned, FSSH has the advantages of path-branching and detailed balance, but by default the algorithm completely ignores all Berry force effects.[9] Moreover, the complex-valued nature of the derivative coupling vector renders the entire FSSH momentum rescaling scheme ambiguous: how can one rescale momentum in a complex direction in any stable sense? Our preliminary studies of FSSH[29,30] have found that choosing a rescaling direction can be crucial as far as achieving accurate results, but that finding such an optimal direction can be very difficult. In particular, in Ref. 29, we assessed three different means of choosing a rescaling direction, and we found that none of them was optimal. For the moment, we have no guidance from any rigorous theory (e.g., the quantum–classical Liouville equation[31,32]) as far as choosing a rescaling direction. Note that, to our knowledge, no one has (as of yet) applied AIMS to a problem with a complex-valued Hamiltonian, though this represents a very interesting future research direction (see Sec. IV).

Despite these fundamental theoretical limitations, after exploring complex-valued semiclassical problems empirically for several years,[9,29,30] at this point, our research group does have some empirical intuition as to what criteria must be satisfied by an appropriate FSSH rescaling scheme. For instance, we have learned that, whenever benchmarking FSSH in multiple dimensions in the presence of a Berry phase, it is crucial to assess performance both via transition probabilities and via nuclear velocities. Moreover, we have developed a set of model problems that will stringently test any *ad hoc* proposed correction to the FSSH protocol.

With this background in mind, in the present paper, we will present what we believe to be a robust extension of Tully's FSSH algorithm as far as modeling the nuclear dynamics through and/or in the vicinity of complex-valued single avoided crossings with two electronic states. After incorporating Berry force into equation of motion, we propose to use a two-dimensional algorithm for momentum rescaling that completely avoids the need for any backtracking[30] (see Sec. IV). For a suite of two-dimensional model systems, our approach has been able to achieve a satisfying accuracy in predicting state-to-state transition probabilities and nuclear momenta. These achievements suggest that an FSSH-inspired approach may soon be able to describe geometric magnetic effects within more realistic nonadiabatic dynamics simulations that closely model experiments.

This paper is organized as follows: in Sec. II, we describe the new algorithm (and in particular our optimized momentum rescaling scheme). In Sec. III, we present the results of our model systems. In Sec. IV, we discuss the implications and limitations of our approach.

II. METHODS

A. The geometry of avoided crossings

We focus on complex-valued avoided crossings between two electronic states. We assume that the adiabatic basis coincides with the diabatic basis asymptotically (outside the crossing region) (see Fig. 1). This confluence defines a "proper" set of diabats (akin to a pointer basis[33,34]). For example, in Tully's first model,[15] the proper diabats are just the diabats given by the author.[35]

We restrict our attention to scattering calculations where the incoming nuclear wavepacket is restricted to a single adiabat (or equivalently a proper diabat[36]). Without loss of generality, we denote the initial diabat as $|a\rangle$; the other diabat (in our two-level system) is denoted as $|b\rangle$. In the basis $|a\rangle$, $|b\rangle$, any two-state Hamiltonian has the following form:

$$H = V\begin{bmatrix} -\cos\theta & e^{-i\phi}\sin\theta \\ e^{i\phi}\sin\theta & \cos\theta \end{bmatrix}, \tag{2}$$

where V, θ, and ϕ are functions of nuclear coordinates. Hamiltonian (2) defines three unique directions: $\mathbf{g} = \nabla V$, $\mathbf{h} = \nabla\theta$, and

$$\mathbf{k} = \nabla\phi - \frac{\nabla\theta(\nabla\theta\cdot\nabla\phi)}{|\nabla\theta|^2}. \tag{3}$$

Below, we will assume the directions of $\mathbf{h}$ and $\mathbf{k}$ and the magnitude of $\mathbf{k}$ can be approximated as constants locally in the crossing region, as in the case of a sharp crossing. Future work will need to assess how the present method will perform (and potentially need to be adjusted) in the case of a conical intersection, where these directions are not constant.

For the most part, one can model the dynamics of the Hamiltonian in Eq. (2) using standard FSSH dynamics. However, a few

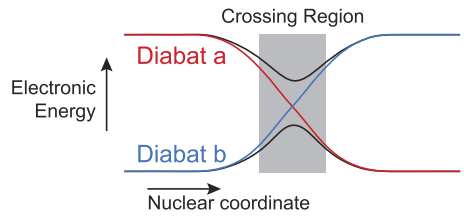

FIG. 1. Definition of "proper" diabatic surfaces (colored curves) for an avoided crossing. The proper diabats asymptotically coincide with adiabats (black curves) outside the crossing.

adjustments are needed to include the complex-valued nature of Eq. (2), as discussed in Secs. II B–II D.

B. FSSH with Berry force

According to the usual FSSH *ansatz*, a nuclear wavepacket is propagated as a swarm of trajectories. Each trajectory moves along a classical path $\mathbf{R}(t)$ on an active surface $n(t)$ with momentum $\mathbf{P}(t)$ and is associated with electronic states $c_j(t), j = 0, 1, \ldots, N_{\text{basis}}$. For a real-valued Hamiltonian, a trajectory on surface j feels the Born–Oppenheimer force ∇E_n. However, for the case of a complex-valued Hamiltonian, following Refs. 29 and 30, we incorporate Berry force effects by adding Eq. (1) to the total force felt by a particle moving along adiabat j. Thus, the quantities $\mathbf{R}$, $\mathbf{P}$, and c_j are updated by

$$\dot{\mathbf{P}} = -\nabla E_n + \frac{2\hbar}{M}\sum_k \text{Im}\{(\mathbf{P}\cdot\mathbf{d}_{kn})\mathbf{d}_{nk}\}, \tag{4}$$

$$\dot{\mathbf{R}} = \frac{\mathbf{P}}{M}, \tag{5}$$

$$\dot{c}_j = -\frac{i}{\hbar}E_j c_j - \frac{1}{M}\sum_k (\mathbf{P}\cdot\mathbf{d}_{jk})c_k, \tag{6}$$

where M is the nuclear mass, E_j is the energy of the adiabatic surface j, and $\mathbf{d}_{jk}$ is the derivative coupling between surface j and k. As described by Tully,[15] the active surface of a trajectory can "hop" to match the population of electronic states. The hopping rate from surface j to surface k is given by

$$g_{j\to k} = \frac{1}{M}\max\left[0, -2\,\text{Re}\left\{\frac{c_k^*}{c_j^*}\mathbf{P}\cdot\mathbf{d}_{kj}\right\}\right]. \tag{7}$$

When a trajectory hops, its momentum will be rescaled for energy conservation. If such a rescaling is impossible, the hop will be forbidden.

C. Rescaling direction

For a real-valued Hamiltonian [i.e., $\phi \equiv 0$ in Hamiltonian (2)], $\mathbf{h}$ is the direction of the derivative coupling and several semiclassical papers have shown that this is the optimal rescaling direction.[32,37–42,71–75] For a complex-valued Hamiltonian, however, there is no relevant semiclassical argument about how to choose a rescaling direction and recent numerical studies have shown that $\mathbf{h}$ does not always yield satisfying results—especially for dynamics with small momenta.[29] Below, we will consider a new protocol for momentum rescaling that performs much better than naively using the $\mathbf{h}$ direction. We will restrict ourselves to Hamiltonian (2) and the geometries specified in Sec. II A. To motivate our scheme, consider the following three scenarios.

1. The adiabatic limit

A trajectory in the adiabatic limit always stays on a single adiabat. For the sake of convenience, we will use the following definition of the adiabats for Hamiltonian (2) here, but note that our results do not depend on the gauge,

$$\begin{aligned}|0\rangle &= \cos\frac{\theta}{2}e^{-i\phi}|a\rangle - \sin\frac{\theta}{2}|b\rangle,\\ |1\rangle &= \sin\frac{\theta}{2}e^{-i\phi}|a\rangle + \cos\frac{\theta}{2}|b\rangle,\end{aligned} \tag{8}$$

where $|a\rangle, |b\rangle$ are the two proper diabats.

Now, let us suppose the trajectory always stays on adiabat $|0\rangle$. From Eq. (1), the Berry force on adiabat $|0\rangle$ is

$$\mathbf{F}_0^B = \frac{2\hbar}{M}\text{Im}\{(\mathbf{P}\cdot\mathbf{d}_{10})\mathbf{d}_{01}\}. \tag{9}$$

If we differentiate Eq. (8), we find $\mathbf{d}_{01} = \frac{1}{2}(\nabla\theta + i\sin\theta\nabla\phi)$, so Eq. (9) expands to

$$\mathbf{F}_0^B = \frac{\hbar}{2M}\sin\theta((\mathbf{P}\cdot\nabla\theta)\nabla\phi - (\mathbf{P}\cdot\nabla\phi)\nabla\theta). \tag{10}$$

Asymptotically, Berry force leads to a momentum change for a transmitted trajectory, denoted as $\mathbf{P}^B$. Among all spatial components of $\mathbf{P}^B$, we are most interested in the component in the $\mathbf{k}$ direction given by Eq. (3). This component can be calculated by integrating Berry force from time 0 to t,

$$\begin{aligned}P_k^B[0;0\to t] &= \int_0^t \hat{\mathbf{k}}\cdot\mathbf{F}_0^B dt\\ &= \int_0^t \frac{\hbar}{2M}\big(\sin\theta(\mathbf{P}\cdot\nabla\theta)(\nabla\phi\cdot\hat{\mathbf{k}}) - (\mathbf{P}\cdot\nabla\phi)(\nabla\theta\cdot\hat{\mathbf{k}})\big)dt.\end{aligned} \tag{11}$$

Here, $\hat{\mathbf{k}} = \mathbf{k}/|k|$ is the normalized direction, and $P_k^B[0;0\to t]$ stands for the k component for $\mathbf{P}^B$ on adiabatic surface $|0\rangle$, which arises from time 0 to t. From Eq. (3), $\nabla\phi\cdot\hat{\mathbf{k}} = |k|$ and $\nabla\theta\cdot\hat{\mathbf{k}} = 0$, and therefore,

$$\begin{aligned}P_k^B[0;0\to t] &= \int_0^t \frac{\hbar}{2M}\sin\theta(\mathbf{P}\cdot\nabla\theta)|k|dt\\ &= \int_0^t \frac{\hbar}{2}\sin\theta(\dot{\mathbf{R}}\cdot\nabla\theta)|k|dt.\end{aligned} \tag{12}$$

Using the chain rule for differentiation, we further find

$$\begin{aligned}P_k^B[0;0\to t] &= \int_0^{\mathbf{R}_t}\frac{\hbar}{2}\sin\theta(d\mathbf{R}\cdot\nabla\theta)|k|\\ &= \int_0^{\theta(\mathbf{R}_t)}\frac{\hbar}{2}|k|\sin\theta d\theta\\ &= \left(\sin^2\frac{\theta(\mathbf{R}_t)}{2} - \sin^2\frac{\theta(\mathbf{R}_0)}{2}\right)\hbar|k|.\end{aligned} \tag{13}$$

From Eq. (8), we find $\sin^2\frac{\theta(\mathbf{R})}{2} = |\langle b|0(\mathbf{R})\rangle|^2$, and therefore,

$$P_k^B[0;0\to t] = \left(|\langle b|0(\mathbf{R}_t)\rangle|^2 - |\langle b|0(\mathbf{R}_0)\rangle|^2\right)\hbar|k|. \tag{14}$$

Following the same derivation as in Eqs. (9)–(13), we can also find P_k^B for adiabat $|1\rangle$ as follows:

$$P_k^B[1;0\to t] = \left(|\langle b|1(\mathbf{R}_t)\rangle|^2 - |\langle b|1(\mathbf{R}_0)\rangle|^2\right)\hbar|k|. \tag{15}$$

Physically speaking, the change in the asymptotic momentum is proportional to the change in the population projected onto a certain diabat. Note that the labeling between diabat $|a\rangle$ and $|b\rangle$ is arbitrary and Eqs. (14) and (15) will always be held valid as long as ϕ is defined as the phase of $\langle b|H|a\rangle$ [as in Hamiltonian (2)].

2. The diabatic limit

In FSSH, a trajectory in the extreme diabatic limit hops once between adiabats and ends up moving along with the same diabat as it started on. Here, we suppose the initial adiabat is $|0\rangle$ and the final adiabat is $|1\rangle$. In the diabatic limit, the wavepacket should not feel any Berry force, so the overall asymptotic momentum $\mathbf{P}^B$ (and its individual components) should be zero. However, in practice, since FSSH randomizes the hopping position, the accumulation of Berry force on the two surfaces might not cancel, i.e., there is no guarantee that we will find $\mathbf{P}^B = 0$ in practice. To ensure the vanishing of the asymptotic momentum, we should add a momentum correction $\Delta\mathbf{P}$ whenever a trajectory hops. Mathematically, if a hop occurs at time t_1, $\Delta\mathbf{P}$ should be a vector in the $\mathbf{h}-\mathbf{k}$ plane and satisfy

$$\mathbf{P}^B[0; 0 \to t_1] + \Delta\mathbf{P} + \mathbf{P}^B[1; t_1 \to \infty] = 0. \tag{16}$$

As above, let us consider the $\mathbf{k}$ component of $\Delta\mathbf{P}$. Using Eqs. (14) and (15), we find

$$\begin{aligned}\Delta P_k &= -P_k^B[0; 0 \to t_1] - P_k^B[1; t_1 \to \infty] \\ &= -\left(|\langle b|0(\mathbf{R}_{t_1})\rangle|^2 - |\langle b|0(\mathbf{R}_0)\rangle|^2\right)\hbar|k| \\ &\quad - \left(|\langle b|1(\mathbf{R}_\infty)\rangle|^2 - |\langle b|1(\mathbf{R}_{t_1})\rangle|^2\right)\hbar|k|.\end{aligned} \tag{17}$$

Finally, if the trajectory is transmitted and both the initial position $\mathbf{R}_0$ and the final position $\mathbf{R}_\infty$ are sufficiently outside the crossing region, we can assume $|\langle b|0(\mathbf{R}_0)\rangle|^2 = |\langle b|1(\mathbf{R}_\infty)\rangle|^2$ (see Fig. 1 for an intuitive view). Therefore, Eq. (17) reduces to

$$\Delta P_k = \left(|\langle b|1(\mathbf{R}_{t_1})\rangle|^2 - |\langle b|0(\mathbf{R}_{t_1})\rangle|^2\right)\hbar|k|. \tag{18}$$

Note the similarity between Eqs. (12) and (18).

3. The frustrated case

Often a trajectory does not have sufficient energy to hop, and the result is a frustrated or a forbidden hop. Now, within standard FSSH for real-valued Hamiltonians, momentum rescaling is in the $\mathbf{h}$ direction. Vice versa, in the presence of a Berry force, which leads to an asymptotic momentum correction, one presumes that the momentum rescaling scheme should become

$$\mathbf{P} \to \mathbf{P} + \Delta P_k\hat{\mathbf{k}} + \alpha\mathbf{h}. \tag{19}$$

During our preliminary study, empirically we have found that strictly enforcing Eq. (19) underestimates the hopping probability because doing so often precludes forbids some hops that can succeed without the inclusion of a Berry force or momentum correction at all. Therefore, for a hop that cannot be rescaled by Eq. (19), we propose to add an additional test to see if the hop can succeed by rescaling according to a calculation that completely ignores the Berry force and momentum correction effects. Mathematically, we check if

$$\mathbf{P}^{\text{test}} = \mathbf{P} - \mathbf{P}^B + \alpha\mathbf{h} = \mathbf{P} - P_k^B\hat{\mathbf{k}} - P_h^B\mathbf{h} + \alpha\mathbf{h} \tag{20}$$

can serve as a rescaling direction. By defining $\beta = \alpha - P_h^B$, Eq. (20) becomes

$$\mathbf{P}^{\text{test}} = \mathbf{P} - P_k^B\hat{\mathbf{k}} + \beta\mathbf{h}. \tag{21}$$

We will check whether β as determined by energy conservation has a real-valued solution. If β has a solution, the hop should be allowed. In this case, we set the $\mathbf{h}$ component of the momentum to 0 and the $\mathbf{k}$ component as close to our target value as possible without breaking energy conservation.

4. Outline of new rescaling scheme

We can now summarize our proposed algorithm for choosing a rescaling direction for FSSH hop from adiabat n to adiabat n'. We assume that a given trajectory is initialized on one proper diabat $|\zeta\rangle \in \{|a\rangle, |b\rangle\}$ and that all nonadiabatic effects arise later in time when the trajectory approaches a crossing.

Step 1: Diabatize the Hamiltonian and ensure that the diabats $|a\rangle$ and $|b\rangle$ are proper diabats. This may be difficult in practice, but one can argue that performing localized diabatization can be related to calculating the stable states of one small electronic system inside of a bath of solvent.[43] Calculate $\mathbf{h}$ and $\mathbf{k}$ according to Eqs. (2) and (3).

Step 2: If a hop is allowed energetically, rescale the momentum by

$$\mathbf{P}^{\text{new}} = \mathbf{P} + \left(\left|\langle b|n'\rangle\right|^2 - |\langle b|n\rangle|^2\right)\hbar\mathbf{k} + \alpha\mathbf{h}, \tag{22}$$

where α is determined by energy conservation,

$$\left|\mathbf{P}^{\text{new}}\right|^2 = |\mathbf{P}|^2 + 2M(E_n - E_{n'}). \tag{23}$$

Here, one must be careful about signs and insist $\phi \equiv \arg\langle b|H|a\rangle$. If there is a real-valued solution for α, we choose that solution with the smallest norm and we are done.

Step 3: Assuming we have failed on Step 2, set

$$\mathbf{P}^{\text{test}} = \mathbf{P} - \left(|\langle b|n\rangle|^2 - |\langle b|\zeta\rangle|^2\right)\hbar\mathbf{k} + \beta\mathbf{h}. \tag{24}$$

Then, solve for β that satisfies energy conservation, i.e., $\left|\mathbf{P}^{\text{test}}\right|^2 = |\mathbf{P}|^2 + 2M(E_n - E_{n'})$. This test checks whether a hop would be allowed if we had not included Berry force. If there is no solution for β, the hop is forbidden and we go to Step 4. Otherwise, set

$$\mathbf{P}^{\text{new}} = \mathbf{P} - \frac{\mathbf{P}\cdot\mathbf{h}}{|h|^2}\mathbf{h} + \gamma\hbar\mathbf{k}. \tag{25}$$

Note that, at this point, γ is mathematically guaranteed to have a real-valued solution; among the pair of solutions, choose the γ that is closest to $\left(\left|\langle b|n'\rangle\right|^2 - |\langle b|n\rangle|^2\right)$.

Step 4: Historically, there has been a large debate about whether or not to reverse velocities upon a frustrated hop[44–47] from state n to state n'. To date, the emerging consensus is that one can recover erroneous small transmission probabilities if one reverses velocities provided the the energy gradient of state

n' does not oppose the current motion. By contrast, one can recover erroneously large transmission probabilities if one does not reverse velocities and the gradient of state n' does oppose the current velocity (as often occurs in the spin-boson model). Thus, in general, the best approach follows the rule of Jasper and Truhlar,[48,49] such that if a hop is rejected, the trajectory's momentum is reversed if

$$(\nabla E_{n'} \cdot \mathbf{h})(\mathbf{P} \cdot \mathbf{h}) > 0. \tag{26}$$

Finally, note that when the Hamiltonian is real-valued, $\mathbf{k}$ is always 0 and both Eqs. (22) and (24) reduce to $\mathbf{P}^{\text{new}} = \mathbf{P} + \alpha\mathbf{h}$, and therefore, the momentum rescaling reduces to the fashion of standard FSSH.

D. Decoherence

There is a long history to understanding decoherence with FSSH calculations, going back to early work by Rossky, Truhlar, Hammes-Schiffer, and others.[19–21,50–54] In general, it has long been appreciated that a decoherence correction is required when trajectories on different adiabatic surfaces emerge from a crossing with different forces and split in different directions.

Below, when modeling dynamics for the Hamiltonian in [Eqs. (27)–(29)], we have found that decoherence is important. To that end, rather than using an involved decoherence scheme designed for a real-valued Hamiltonian[50,55–59] (which may or may not be applicable for the case of a complex-valued Hamiltonian, see Sec. IV), we will employ the very simplest (yet effective) decoherence scheme possible for the elementary scattering calculations below, which is very similar to the approach suggested by Fang and Hammes-Schiffer.[53] Namely, if n is the active adiabatic state, we will collapse the amplitudes by setting $c_j \to \delta_{nj}$ if we find $(\mathbf{P} \cdot \mathbf{h})(\mathbf{P}_{t=0} \cdot \mathbf{h}) < 0$. A trajectory can decohere only once in the scattering calculations below.

Note that, for a real-valued Hamiltonian, it is known that decoherence effects emerge only when particles pass through the same crossing more than once.[60,61] Thus, provided decoherence emerges

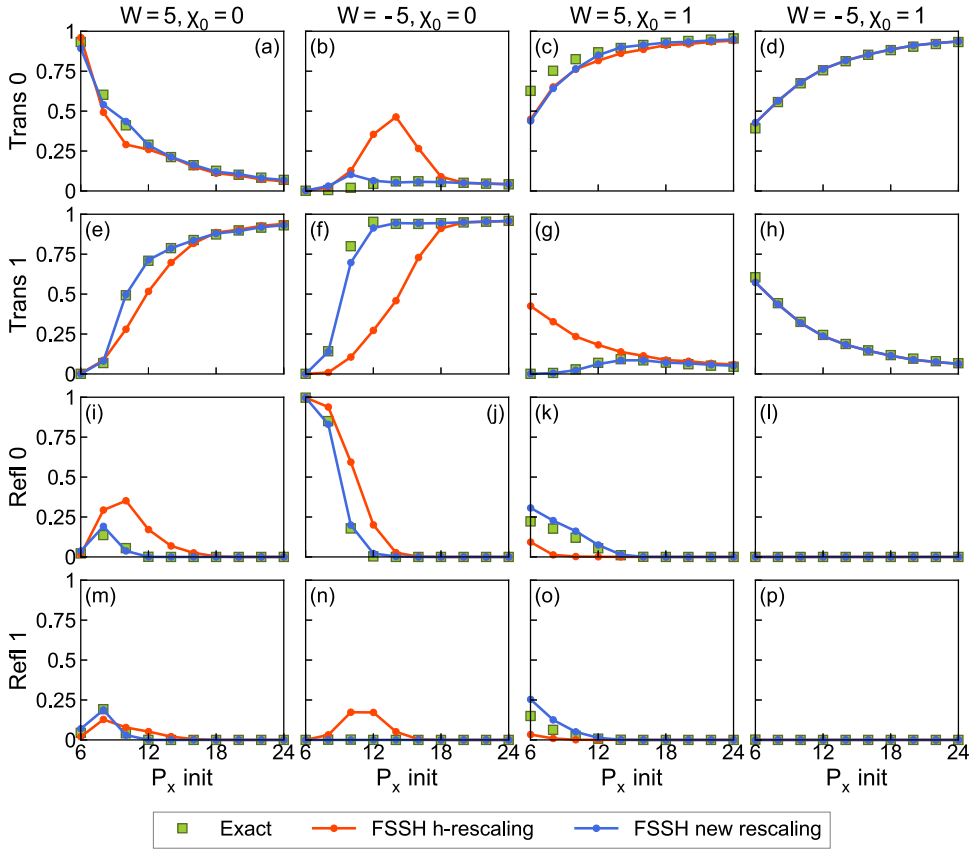

FIG. 2. State-to-state probabilities to transmit and reflect starting on different adiabats and with different W values. For each column, the initial surface is denoted at the top of the graph as χ_0; we investigate both $|\chi_0\rangle = |0\rangle$ (incoming wavepacket on the lower adiabat) and $|\chi_0\rangle = |1\rangle$ (incoming wavepacket on the upper adiabat). (a), (e), (i), and (m) plot probabilities starting on adiabat 0 with $W = 5$; (b), (f), (j), and (n) plot probabilities starting on adiabat 0 with $W = -5$; (c), (g), (k), and (o) plot probabilities starting on adiabat 1 with $W = 5$; (d), (h), (l), and (p) plot probabilities starting on adiabat 1 with $W = -5$. Note that if run FSSH dynamics with **h**-rescaling, we find there many problems for low incoming momenta. However, if we run FSSH dynamics with our new rescaling schemes, the algorithm provides satisfying results for all initial conditions. Parameters are $A = 0.02$, $B = 3$, and $\alpha = 0$, and for each point, we average over 10^4 trajectories. All calculations include the simple decoherence scheme described in Sec. II D.

for complex-valued Hamiltonians in a manner similar to real-valued Hamiltonians, the present algorithm should suffice for the simple scattering calculations performed below (where effectively each trajectory never goes through a crossing more than twice). For a longer discussion of decoherence, see Sec. IV.

III. RESULTS

In this paper, we parameterize Hamiltonian (2) with two nuclear degrees of freedom x and y. The definitions of V, θ, and ϕ are

$$V(x,y) = A\left(1 - \alpha e^{-B^2x^2}\right), \tag{27}$$

$$\theta(x,y) = \frac{\pi}{2}(\mathrm{erf}(Bx) + 1), \tag{28}$$

$$\phi(x,y) = -Wy. \tag{29}$$

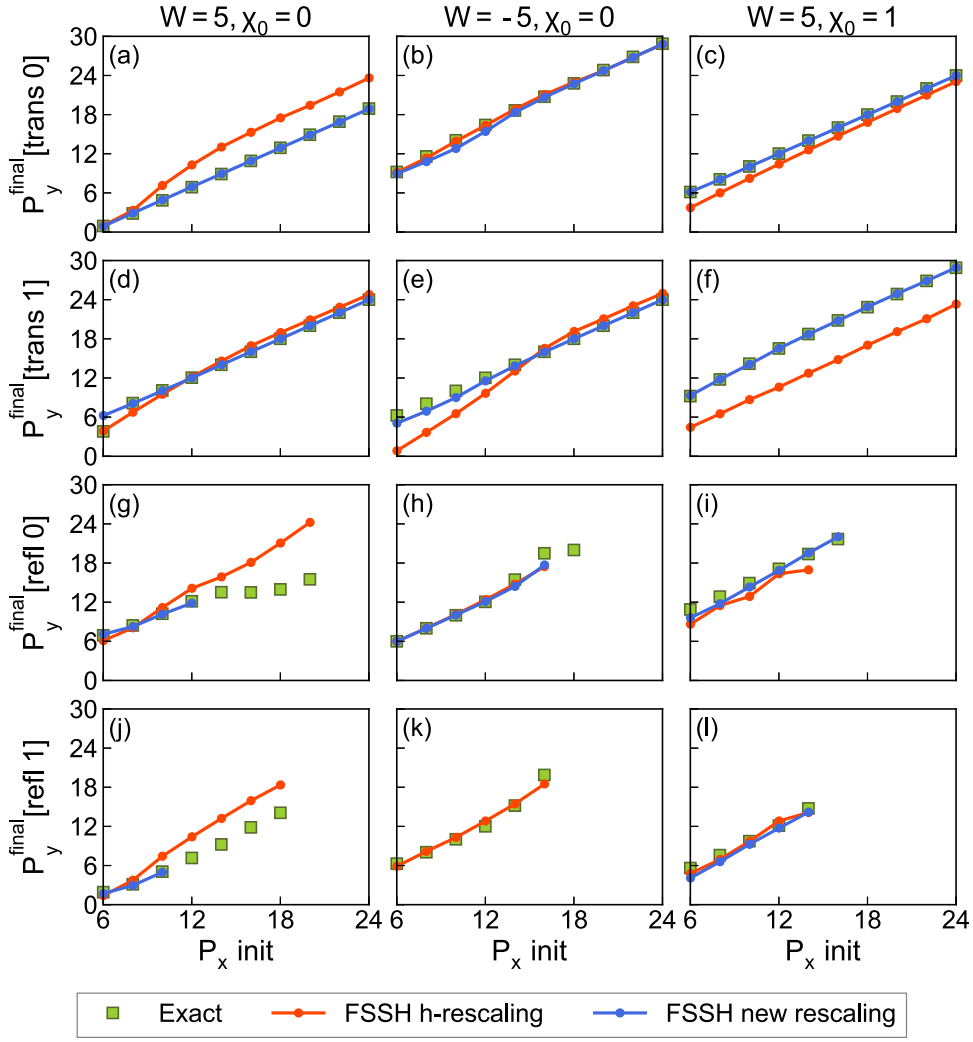

FIG. 3. Average final momentum P_y^{final} on the transmitted and reflected wavepackets according to exact dynamics and FSSH simulations using the same parameters as in Fig. 2. As opposed to Fig. 2, we plot only three columns here (instead of four). (a), (d), (g), and (j) plot probabilities when starting on adiabat 0 with $W = 5$; (b), (e), (h), and (k) plot probabilities when starting on adiabat 0 with $W = -5$; (c), (f), (i), and (l) plot probabilities when starting on adiabat 1 with $W = 5$. Note that, for the case of $W = -5, \chi_0 = 1$, both FSSH rescaling schemes yield accurate (and indistinguishable) results, in agreement with Fig. 2, and so we do not plot such data here. In general, these data show that, although **h**-rescaling often fails to predict the correct momentum, FSSH with our new rescaling scheme works quite well. As a side note, for all FSSH data presented here, we plot $P_y^{\mathrm{final}}[\mathrm{refl}]$ only where there is a meaningful (nonzero) probability of reflection. In particular, in (g) and (j) (when $P_x^{\mathrm{init}} \geq 12$) and in (k) (for all P_x^{init}), the exact probability of reflection is exceedingly small ($< 10^{-5}$) and we do not have enough FSSH trajectories to sample these transitions according to the new rescaling method. By contrast, standard **h**-rescaling incorrectly predicts a large reflection probability (and therefore, one can easily extract a momentum for reflection)—but this prediction is effectively erroneous. See (i), (m), and (n) in Fig. 2.

In this model, $\mathbf{h} = \frac{\partial\theta}{\partial x}\hat{\mathbf{x}}$ and $\mathbf{k} = -W\hat{\mathbf{y}}$. The two adiabatic electronic states are defined as

$$|0\rangle = \left[\cos\frac{\theta}{2}e^{-i\phi}, -\sin\frac{\theta}{2}\right]^T,$$
$$|1\rangle = \left[\sin\frac{\theta}{2}e^{-i\phi}, \cos\frac{\theta}{2}\right]^T, \tag{30}$$

with energy $E_0 = -V(x,y)$ and $E_1 = V(x,y)$.

The initial wave function of the wavepacket is

$$\Psi_0(x,y) = \exp\left\{-\frac{(x-x_0)^2}{\sigma_x^2} - \frac{(y-y_0)^2}{\sigma_y^2} + i\frac{P_x^{\text{init}}}{\hbar}x + i\frac{P_y^{\text{init}}}{\hbar}y\right\}|\chi_0\rangle, \tag{31}$$

where we set $x_0 = -3, y_0 = -3$, $\sigma_x = \sigma_y = 1.0$, and $P_x^{\text{init}} = P_y^{\text{init}}$ and we set the initial electronic state $|\chi_0\rangle$ to either the adiabatic state $|0\rangle$ or $|1\rangle$. The nuclear mass is 1000. All parameters are in atomic units. For the exact quantum dynamics, we use the fast Fourier transform technique[62] with a 768 × 768 grid and a grid spacing of 0.031 25.

For FSSH calculations, the initial positions and momenta for the classical swarm are sampled according to the Wigner distribution, i.e., the position is sampled from a Gaussian distribution centered at (x_0, y_0) with standard deviation $\sigma = (\sigma_x/2, \sigma_y/2)$, and the momentum is sampled from Gaussian distribution centered at $(P_x^{\text{init}}, P_y^{\text{init}})$ with standard deviation $\sigma_P = (\hbar/\sigma_x, \hbar/\sigma_y)$. The eigenvectors used in the FSSH simulations are adjusted on the fly for the "parallel transport" condition (i.e., $\langle j(t)|j(t+dt)\rangle \approx 1$ for $j = 0, 1$). 10^4 trajectories are sampled for each data point.

A. A curve crossing with flat adiabats

For our first test case, we set $A = 0.02$, $B = 3$, and $\alpha = 0$, which corresponds to completely flat adiabatic surfaces. As shown in Fig. 2, we find reflection occurs for many of the systems, especially at low energy. Such reflection is caused by the Lorentz-like Berry force, which turns trajectories around and, for a two-state problem, is a unique signature of a complex-valued Hamiltonian and cannot be described by FSSH without explicitly incorporating Berry force (see Figs. S1 and S2 in the supplementary material). Note that all dynamics are very sensitive to the direction of magnetic force, which is controlled by the sign of W. For example, when starting from adiabat 0 with momentum $P_x^{\text{init}} = 6$, almost all trajectories are reflected when $W = -5$, but trajectories are transmitted when $W = 5$. When we implement our new rescaling algorithm plus a

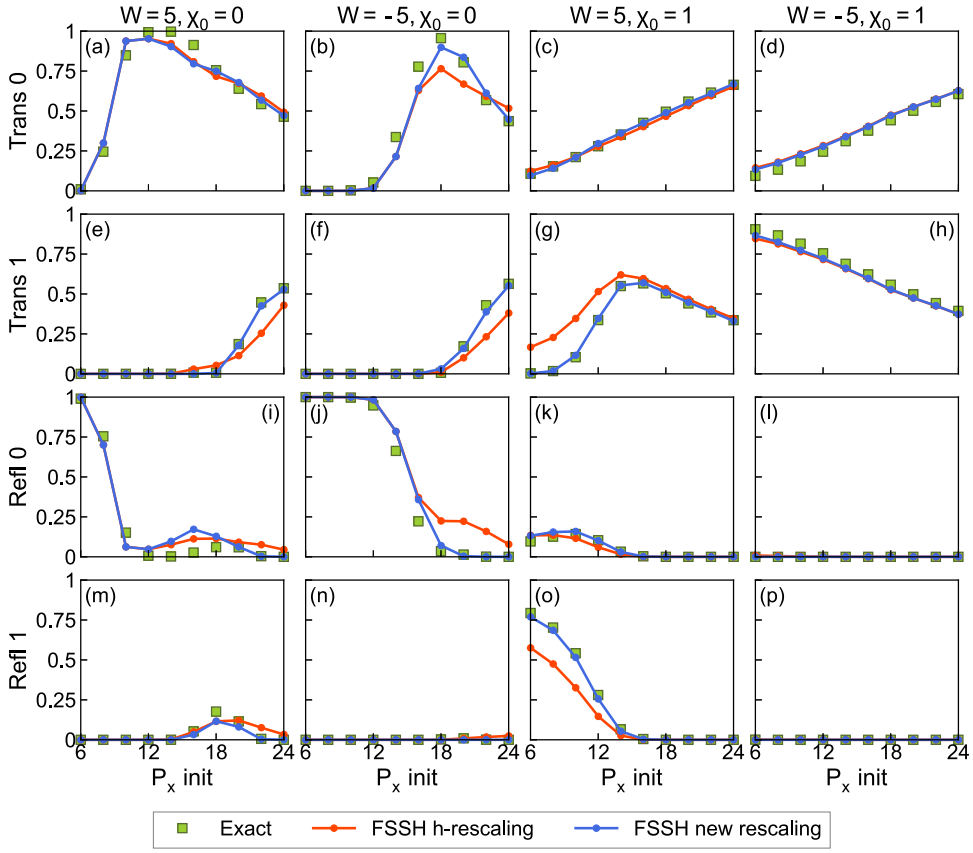

FIG. 4. Same as Fig. 2, except $A = 0.1$ and $\alpha = 0.5$. Here, we benchmark the FSSH algorithm for a model problem with a barrier. For the most part, the new rescaling scheme performs quite well.

simple decoherence correction, all reflection and transmission probabilities are well described by FSSH. That being said, Fig. 2 shows that simply rescaling along **h** (which is the x direction or method 2 from Ref. 29) is not sufficient. Clearly, one must be quite careful when choosing momentum rescaling directions when encountering electronic Hamiltonians with a significant complex-valued nature.

Beyond scattering probabilities, in Fig. 3, we plot the final momentum along the y direction (which is also the **k** direction for our model Hamiltonian). We find that, whenever a transmitting trajectory changes its diabat (or maintains its adiabat), P_y^{final} is shifted $\pm\hbar W$ from the initial momentum, as predicted by Eq. (14). If such a shift is not allowed energetically, the transmission probability dramatically decreases. Using our new rescaling scheme, FSSH does capture this momentum shift. However, as above, when using **h** as the rescaling direction, the FSSH-predicted momentum has a systematic error. As a side note, for trajectories that reflect on the initial adiabat, no hops are required and both FSSH algorithms correctly predict that $P_y^{\text{final}} = P_y^{\text{init}}$ and (not shown) $P_x^{\text{final}} = -P_x^{\text{init}}$.

B. A curve crossing with adiabatic energy barriers

Next, in Fig. 4, we turn to a second model Hamiltonian with $A = 0.1$, $B = 3$, and $\alpha = 0.5$. In Fig. 4, we investigate whether the performance highlighted above is altered by the presence of a barrier; in other words, was the strong performance recorded above in Fig. 2 reliant on the presence of flat adiabats?

To that end, for the present Hamiltonian, with $\alpha = 0.5$, the lower adiabat (adiabat 0) has a barrier. Thus, one might expect that most reflection when a wavepacket starting on the lower adiabat and its x momentum is insufficient to cross the barrier. In our model Hamiltonian with $A = 0.1$ and $\alpha = 0.5$, the barrier should cause reflection when $P_x^{\text{init}} < \sqrt{2MA\alpha} = 10$; however, because of the impact of a magnetic field, there can also be substantial reflection when $|\chi_0\rangle = |0\rangle$, $W = -5$, and $P_x^{\text{init}} = 14$. According to Fig. 4, our algorithm agrees well with exact results for almost all initial conditions.

C. Decoherence

Finally, let us address the effect of decoherence. To make our calculations as interesting as possible, we investigate the case for $\alpha = 0$, such that the adiabats are flat. In such a case, every reasonable (and rigorous) FSSH calculation will predict zero decoherence; after all, the adiabats have the same force.[19,29,50,55,63] However, for a complex-valued Hamiltonian, because of Berry force differences between adiabats, decoherence is possible.

In Fig. 5, we compare the results of FSSH with and without decoherence, in both cases using our new rescaling scheme. We test two systems: $A = 0.02, B = 6, W = 5, \alpha = 0, |\chi_0\rangle = |1\rangle$ and $A = 0.05, B = 3, W = 5, \alpha = 0, |\chi_0\rangle = |0\rangle$. When decoherence is absent, FSSH can predict extremely erroneous results, including the opposite reflection probability on the two adiabats. Clearly, much more research will be needed as far as investigating the nature of decoherence for complex-valued Hamiltonians. See below.

Finally, we find that for the calculations above (Figs. 2–4), decoherence is only helpful for our new rescaling method. For **h**-rescaling, decoherence does not improve (and often degrades) scattering results. The full data with both rescaling methods and without decoherence are provided in the supplementary material.

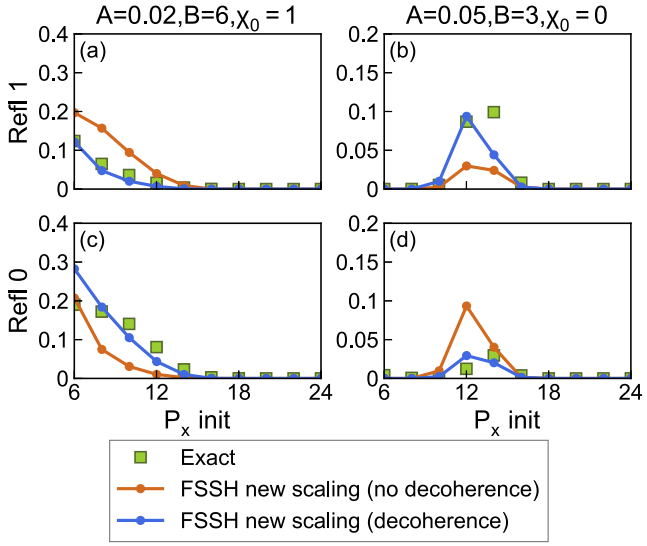

FIG. 5. The state-resolved probability for reflection with $A = 0.02, B = 6, W = 5, \alpha = 0, |\chi_0\rangle = |1\rangle$ [(a) and (c)] and $A = 0.05, B = 3, W = 5, \alpha = 0, |\chi_0\rangle = |0\rangle$ [(b) and (d)]. Here, we plot exact dynamics as well as FSSH according to our new scaling scheme both (i) with and (ii) without decoherence. Note that upon reflection, according to FSSH, the probability to reach a given state is sensitive to decoherence (in agreement with previous results using real-valued Hamiltonians without Berry force effects[61]).

IV. DISCUSSION

We have presented a new rescaling scheme for propagating FSSH dynamics in the presence of a complex-valued Hamiltonian (where Berry force arises). We have tested this algorithm for a multidimensional problem, where both the norm *and* the direction of a trajectory's motion are strongly coupled to electronic transitions. The Hamiltonian in Eq. (2) is quite distinct from standard real-valued Hamiltonians for which each point carries a unique derivative coupling direction and for which the velocity rescaling direction is often not crucial in practice;[64] for the present Hamiltonian, the choice of the rescaling direction is absolutely essential as far as recovering the exact quantum results. We find that, by designing a velocity rescaling scheme so as to recover the correct asymptotic nuclear momenta, we also (almost automatically) gain a huge improvement over previous rescaling schemes as far as the transmission and reflection probabilities; our results here agree surprisingly well with those from exact dynamics. In the end, the strong performance of the current method indicates that Markovian FSSH-level algorithms (or generalizations thereof) may well be sufficient to capture many aspects of geometric phases (and their corresponding magnetic field effects) in nonadiabatic dynamics.[65]

Despite the positive results above, several obstacles remain before the present algorithm can be applied in a realistic setting (e.g.,

with *ab initio* potentials). First, the algorithm in this paper strongly depends on the choice of diabatic basis. Apparently, not all diabatic basis sets are meaningful—for example, in the basis $\frac{|a\rangle+|b\rangle}{\sqrt{2}}$, $\frac{|a\rangle-|b\rangle}{\sqrt{2}}$, Hamiltonian (2) reads

$$H' = V\begin{bmatrix} \cos\phi\sin\theta & -\cos\theta + i\sin\phi\sin\theta \\ -\cos\theta - i\sin\phi\sin\theta & -\cos\phi\sin\theta \end{bmatrix}, \tag{32}$$

where the definitions of **h** and **k** are completely different from what we defined in Sec. II. In the current paper, we presume that we have access to a set of proper diabats, or a pointer basis; finding such a basis would appear simple enough for avoided crossings but might be ambiguous in other systems, e.g., Tully's third problem or conical intersections. In such systems, the definition of "proper diabats" may not be unique, and the optimal means of choosing proper diabats for momentum rescaling is not clear. Should the proper diabats depend on the initial position, can they be determined on the fly? There are many questions here.

Second, for the Hamiltonian parameterized by Eqs. (27)–(29), there is only a single crossing seam in our model system and the nuclear wavepackets are sufficiently separated after the scattering process. For systems with more than one crossings, such as Tully's second problem,[15] wavepackets may experience recoherence, i.e., recombination after bifurcating onto different electronic states. Since the origin of Berry force is closely related to electronic coherence, when wavepacket carrying different phases are mixed, the influence of Berry force may be more complicated. Moreover, we must emphasize that the model Hamiltonian above is quite unique in the sense that $\mathbf{h} = \nabla\theta$ (i.e., the effective reaction coordinate) points in a well-defined direction globally. More generally, **h** might not be in a single direction, e.g., in the case of a conical intersection. In such a case, Eq. (14) is no longer exact. In short, looking forwardly and thinking about coherence, there are many reasons why the accuracy of our rescaling scheme needs to be checked.

Third, apart from the issues of recoherence, the data above suggest that we will also need a new view of decoherence. In the standard picture of decoherence, decoherence arises from the difference in forces on different adiabatic states that eventually causes the wavepackets to separate. In Fig. 5, we found that because of Berry force, decoherence may also occur in a system where the adiabats are completely flat. Such a mechanism for decoherence is more complicated than the usual adiabatic decoherence, since at least two degrees of freedom are required to produce a magnetic field. Most importantly, for a system where there are differences in both the adiabatic forces and Berry forces, we do not yet know whether the two forces can be added together or whether they suppress each other. In the end, the concepts of recoherence and decoherence may be more complicated with complex-valued Hamiltonians, and the existing decoherence schemes[19–21,52–54] will also need to be validated in complex-valued Hamiltonians.

Finally, we still lack an effective algorithm for systems with more than two electronic states. The presented algorithm was designed explicitly for a two-state system where all crossings are pairwise, which is the most common case in molecular systems. However, there are many cases where three and more states cross together with different characteristic directions—for example, for a singlet–triplet crossing, the triplet consists of three degenerate states instead of one, and they can interact differently with the singlet.[66] For these systems, the notion of geometric magnetic fields is different and more complicated (for example, there might be contributions from the non-Abelian Berry curvature[66]) and we can anticipate that extending the present algorithm, which relies on the existence of proper diabats and intuitive rescaling schemes, may be more difficult.

Clearly, many obstacles remain as far as developing a robust and reliable, fully general surface hopping algorithm. Nevertheless, the present work opens up the exciting possibility of eventually exploring larger systems with geometric magnetic effects using semiclassical algorithms. To date, semiclassical simulations of electron transfer and electronic relaxation have exclusively ignored Berry force effects. However, these effects may well underlie several spin-related physical and chemical processes, including magnetic field effects in chemical dynamics and chirality induced spin selectivity.[13,67,68]

V. CONCLUSION

In summary, we have developed a new momentum rescaling scheme for FSSH dynamics in the presence of complex-valued Hamiltonians. For certain classes of two-dimensional, single avoided crossings, our algorithm gives satisfying statewise transition probabilities. While the present study will need to be generalized to treat more complicated dynamics (e.g., Hamiltonians with more than two electronic states, more than two crossings, more than two nuclear dimensions, etc.), the results presented here suggest that, when properly constructed, semiclassical FSSH algorithms do have the capability to capture geometric phase effects in non-adiabatic dynamics with strong accuracy. Moreover, we mention that, within AIMS,[16,17] whenever a mother wavepacket comes to a crossing, she requires a momentum for spawning a daughter wavepacket; one must wonder whether the present schemes (presented above) might serve as that optimal direction. Clearly, we have a lot more to learn as we inevitably merge nonadiabatic theory with spin dynamics. However, there is clearly a lot of hope that semiclassical dynamics may soon be applied to models of large molecular systems where the mechanism behind various spin-related physical and chemical reactions remains a matter of debate.[69,70]

SUPPLEMENTARY MATERIAL

See the supplementary material for additional FSSH data demonstrating the effect of operating with different rescaling directions, with or without decoherence .

ACKNOWLEDGMENTS

This material is based on the work supported by the National Science Foundation under Grant No. CHE-2102402.

DATA AVAILABILITY

The data that support the findings of this study are available from the corresponding author upon reasonable request.

REFERENCES

[1] B. Lengsfield and D. R. Yarkony, Adv. Chem. Phys. **82**, 1 (1992).
[2] M. Richter, S. Mai, P. Marquetand, and L. González, Phys. Chem. Chem. Phys. **16**, 24423 (2014).

[3]S. Mai, P. Marquetand, and L. González, Wiley Interdiscip. Rev.: Comput. Mol. Sci. **8**, e1370 (2018).
[4]S. Mai and L. González, Angew. Chem., Int. Ed. **59**, 16832 (2020).
[5]J. C. Tully, Faraday Discuss. **110**, 407 (1998).
[6]W. H. Miller, J. Chem. Phys. **136**, 210901 (2012).
[7]M. Berry and J. Robbins, Proc. R. Soc. London, Ser. A **442**, 659 (1993).
[8]K. Takatsuka, J. Phys. Chem. A **111**, 10196 (2007).
[9]J. Subotnik, G. Miao, N. Bellonzi, H.-H. Teh, and W. Dou, J. Chem. Phys. **151**, 074113 (2019).
[10]Y. Wu, G. Miao, and J. E. Subotnik, J. Phys. Chem. A **124**, 7355 (2020).
[11]Y. Wu and J. E. Subotnik, Nat. Commun. **12**, 700 (2021).
[12]B. Gohler, V. Hamelbeck, T. Z. Markus, M. Kettner, G. F. Hanne, Z. Vager, R. Naaman, and H. Zacharias, Science **331**, 894 (2011).
[13]R. Naaman and D. H. Waldeck, Annu. Rev. Phys. Chem. **66**, 263 (2015).
[14]A. D. McLachlan, Mol. Phys. **8**, 39 (1964).
[15]J. C. Tully, J. Chem. Phys. **93**, 1061 (1990).
[16]M. Ben-Nun, J. Quenneville, and T. J. Martínez, J. Phys. Chem. A **104**, 5161 (2000).
[17]M. Ben-Nun and T. J. Martínez, Adv. Chem. Phys. **121**, 439 (2002).
[18]G. Granucci, M. Persico, and G. Spighi, J. Chem. Phys. **137**, 22A501 (2012).
[19]C. Zhu, S. Nangia, A. W. Jasper, and D. G. Truhlar, J. Chem. Phys. **121**, 7658 (2004).
[20]M. J. Bedard-Hearn, R. E. Larsen, and B. J. Schwartz, J. Chem. Phys. **123**, 234106 (2005).
[21]R. E. Larsen, M. J. Bedard-Hearn, and B. J. Schwartz, J. Phys. Chem. B **110**, 20055 (2006).
[22]P. V. Parandekar and J. C. Tully, J. Chem. Phys. **122**, 094102 (2005).
[23]J. R. Schmidt, P. V. Parandekar, and J. C. Tully, J. Chem. Phys. **129**, 044104 (2008).
[24]T. J. Penfold, E. Gindensperger, C. Daniel, and C. M. Marian, Chem. Rev. **118**, 6975 (2018).
[25]S. J. Cotton, K. Igumenshchev, and W. H. Miller, J. Chem. Phys. **141**, 084104 (2014).
[26]C.-Y. Hsieh and R. Kapral, J. Chem. Phys. **137**, 22A507 (2012).
[27]E. R. Dunkel, S. Bonella, and D. F. Coker, J. Chem. Phys. **129**, 114106 (2008).
[28]P. Huo and D. F. Coker, J. Chem. Phys. **137**, 22A535 (2012).
[29]G. Miao, N. Bellonzi, and J. Subotnik, J. Chem. Phys. **150**, 124101 (2019).
[30]G. Miao, X. Bian, Z. Zhou, and J. Subotnik, J. Chem. Phys. **153**, 111101 (2020).
[31]C. C. Martens and J.-Y. Fang, J. Chem. Phys. **106**, 4918 (1997).
[32]R. Kapral and G. Ciccotti, J. Chem. Phys. **110**, 8919 (1999).
[33]W. H. Zurek, Phys. Rev. D **24**, 1516 (1981).
[34]A. W. Jasper, C. Zhu, S. Nangia, and D. G. Truhlar, Faraday Discuss. **127**, 1 (2004).
[35]Note that for many two-state systems involving ISC, it should be reasonably simple to construct (approximately) such diabats: one can in principle use the electronic states that arise by diagonalizing the Hamiltonian *without* spin-orbit coupling.
[36]Note that, in the presence of a complex-valued Hamiltonian, initialization of a wavepacket on an adiabatic surface is not well-defined because of electronic phase ambiguity.
[37]One might wonder if it is correct to rescale *all* trajectories in the same direction, given that semiclassically a quantum wavepacket needs to be reconstructed by averaging over many classical trajectories. Nevertheless, the scattering formalism of Herman[39] and the QCLE work of Kapral[32,41] make clear that, for a real-valued Hamiltonian, momentum rescaling in the **h**-direction is the right choice for every trajectory here. Furthermore, because all trajectories are propagated independently within an FSSH formalism, such a universal choice of rescaling is the most natural and the only efficient means of ensuring that the asymptotic momentum (post-crossing) is correct (without allowing for interacting trajectories[71]). There is also a large literature demonstrating that, by using electron translation factors[72] to modify the direction of the derivative coupling,[73–75] one can be sure that total momentum conservation is maintained after a nonadiabatic hop.
[38]R. K. Preston and J. C. Tully, J. Chem. Phys. **54**, 4297 (1971).
[39]M. F. Herman, J. Chem. Phys. **81**, 754 (1984).
[40]J. C. Tully, Int. J. Quantum Chem. **40**, 299 (1991).
[41]S. Nielsen, R. Kapral, and G. Ciccotti, J. Chem. Phys. **112**, 6543 (2000).
[42]J. E. Subotnik, W. Ouyang, and B. R. Landry, J. Chem. Phys. **139**, 214107 (2013).
[43]J. E. Subotnik, R. J. Cave, R. P. Steele, and N. Shenvi, J. Chem. Phys. **130**, 234102 (2009).
[44]S. Hammes-Schiffer and J. C. Tully, J. Chem. Phys. **101**, 4657 (1994).
[45]D. F. Coker and L. Xiao, J. Chem. Phys. **102**, 496 (1995).
[46]U. Müller and G. Stock, J. Chem. Phys. **107**, 6230 (1997).
[47]A. W. Jasper, M. D. Hack, and D. G. Truhlar, J. Chem. Phys. **115**, 1804 (2001).
[48]A. W. Jasper and D. G. Truhlar, Chem. Phys. Lett. **369**, 60 (2003).
[49]A. W. Jasper and D. G. Truhlar, "Non-Born-Oppenheimer molecular Dynamics for conical intersections, avoided crossings, and weak interactions," Advanced Series in Physical Chemistry Vol. 17 (World Scientific, 2011), ISBN: 978-981-4313-44-5 978-981-4313-45-2, pp. 375–414.
[50]O. V. Prezhdo and P. J. Rossky, J. Chem. Phys. **107**, 825 (1997).
[51]E. R. Bittner and P. J. Rossky, J. Chem. Phys. **107**, 8611 (1997).
[52]J.-Y. Fang and S. Hammes-Schiffer, J. Chem. Phys. **110**, 11166 (1999).
[53]J.-Y. Fang and S. Hammes-Schiffer, J. Phys. Chem. A **103**, 9399 (1999).
[54]A. W. Jasper and D. G. Truhlar, J. Chem. Phys. **123**, 064103 (2005).
[55]B. J. Schwartz, E. R. Bittner, O. V. Prezhdo, and P. J. Rossky, J. Chem. Phys. **104**, 5942 (1996).
[56]Y. L. Volobuev, M. D. Hack, M. S. Topaler, and D. G. Truhlar, J. Chem. Phys. **112**, 9716 (2000).
[57]M. D. Hack and D. G. Truhlar, J. Chem. Phys. **114**, 2894 (2001).
[58]K. F. Wong and P. J. Rossky, J. Chem. Phys. **116**, 8418 (2002).
[59]K. F. Wong and P. J. Rossky, J. Chem. Phys. **116**, 8429 (2002).
[60]I. Horenko, C. Salzmann, B. Schmidt, and C. Schütte, J. Chem. Phys. **117**, 11075 (2002).
[61]J. E. Subotnik and N. Shenvi, J. Chem. Phys. **134**, 244114 (2011).
[62]D. Kosloff and R. Kosloff, J. Comput. Phys. **52**, 35 (1983).
[63]G. Granucci and M. Persico, J. Chem. Phys. **126**, 134114 (2007).
[64]M. S. Topaler, T. C. Allison, D. W. Schwenke, and D. G. Truhlar, J. Phys. Chem. A **102**, 1666 (1998).
[65]Note that, in a previous communication, we argued that, in order to accurately solve for the correct asymptotic momentum, one might need to implement a non-Markovian "backtracking" adjustment to FSSH in order to account for double or multiple hops.[30] Here, however, we found that such a backtracking correction is completely unnecessary – provided that one chooses the proper the rescaling scheme.
[66]X. Bian, Y. Wu, H.-H. Teh, Z. Zhou, H.-T. Chen, and J. E. Subotnik, J. Chem. Phys. **154**, 110901 (2021).
[67]U. E. Steiner and T. Ulrich, Chem. Rev. **89**, 51 (1989).
[68]P. J. Hore and H. Mouritsen, Annu. Rev. Biophys. **45**, 299 (2016).
[69]M. S. Zöllner, S. Varela, E. Medina, V. Mujica, and C. Herrmann, J. Chem. Theory Comput. **16**, 2914 (2020).
[70]M. S. Zöllner, A. Saghatchi, V. Mujica, and C. Herrmann, J. Chem. Theory Comput. **16**, 7357 (2020).
[71]C. C. Martens, J. Phys. Chem. Lett. **7**, 2610 (2016).
[72]E. Deumens, A. Diz, R. Longo, and Y. Öhrn, Rev. Mod. Phys. **66**, 917 (1994).
[73]J. B. Delos, Rev. Mod. Phys. **53**, 287 (1981).
[74]L. F. Errea, C. Harel, H. Jouini, L. Méndez, B. Pons, and A. Riera, J. Phys. B: At., Mol. Opt. Phys. **27**, 3603 (1994).
[75]S. Fatehi and J. E. Subotnik, J. Phys. Chem. Lett. **3**, 2039 (2012).